Plasma density measurements using chirped pulse broad-band Raman amplification

G. Vieux, B. Ersfeld, J. P. Farmer, M. S. Hur, R. C. Issac et al.

Citation: Appl. Phys. Lett. **103**, 121106 (2013); doi: 10.1063/1.4821581
View online: http://dx.doi.org/10.1063/1.4821581
View Table of Contents: http://apl.aip.org/resource/1/APPLAB/v103/i12
Published by the AIP Publishing LLC.

Plasma density measurements using chirped pulse broad-band Raman amplification

G. Vieux,[1,a)] B. Ersfeld,[1] J. P. Farmer,[1] M. S. Hur,[2] R. C. Issac,[1] and D. A. Jaroszynski[1,b)]
[1]*Scottish Universities Physics Alliance and University of Strathclyde, Glasgow G4 0NG, United Kingdom*
[2]*UNIST, Banyeon-ri 100. Ulju-gun, Ulsan 689-798, South Korea*

(Received 29 April 2013; accepted 1 September 2013; published online 18 September 2013)

Stimulated Raman backscattering is used as a non-destructive method to determine the density of plasma media at localized positions in space and time. By colliding two counter-propagating, ultra-short laser pulses with a spectral bandwidth larger than twice the plasma frequency, amplification occurs at the Stokes wavelengths, which results in regions of gain and loss separated by twice the plasma frequency, from which the plasma density can be deduced. By varying the relative delay between the laser pulses, and therefore the position and timing of the interaction, the spatio-temporal distribution of the plasma density can be mapped out. © *2013 AIP Publishing LLC*. [http://dx.doi.org/10.1063/1.4821581]

Investigations of how intense laser pulses interact with plasma are leading to wide range of high impact applications that include the development of high energy particle accelerators, inertial confinement fusion, and the use of particle beams in health care. Many of these applications require detailed knowledge of the spatial and temporal distribution of the density of plasma media. Numerous methods already exist for determining the plasma density, such as the Langmuir probe,[1] interferometric and spectroscopic techniques, Thomson scattering,[2] etc., but they all have some disadvantages, such as low signal to noise ratio, limited spatial resolution, restrictions to the measurement of average density, relative complexity, assumptions of symmetry, extended computation effort to retrieve the density, etc. Raman backward (RBS) and Raman forward (RFS) scattering are commonly used to determine the density in underdense plasma in studies of laser wakefield accelerators.[3,4] However, they have the disadvantage that they can only measure the integrated density along a beam path and not the localized density; the laser intensity must be sufficiently high to stimulate Raman scattering; density values are difficult to determine if the laser beam ionises the gas to form the plasma, because of ionisation induced spectral blue-shifting. A technique based on simultaneously measuring RBS and RFS spectra has been proposed to obtain both the temperature and plasma density.[5]

In this letter, we propose a method of determining the plasma density based on broad-bandwidth Raman amplification using ultra-short pulses, which allows spatio-temporal measurement of the density with high resolution. Determining the spatial and temporal evolution of the plasma density deep inside a plasma medium is usually difficult or impossible to make using traditional techniques. Our proposed method has several advantages over other methods: e.g. (i) it provides a non invasive tool for determining the electron density and therefore the plasma remains essentially unperturbed, (ii) the density is measured locally and at a fixed time relative to the evolving plasma distribution, and (iii) the plasma density is determined directly and does not require extended calculations.

RBS is a three-wave parametric instability where an incident electromagnetic (EM) wave $(\omega_0, \vec{k_0})$ resonantly decays into a backscattered EM wave $(\omega_1, \vec{k_1})$ and a plasma wave $(\omega_p, \vec{k_p})$ that satisfy the resonance (energy and momentum conservation) conditions $\omega_0 = \omega_1 + \omega_p$ and $\vec{k_0} = \vec{k_1} + \vec{k_p}$, where ω_i and $\vec{k_i}$ represent the frequency and wave vector of the respective waves.[6] A seed pulse injected into a column of under-dense plasma can be amplified by a counter-propagating pump pulse if it is red detuned by the plasma frequency to produce a beat wave that resonantly excites a plasma wave. In the linear RBS regime, the amplitude of the seed grows exponentially as $g = e^{\gamma_0 t}$, where γ_0 is the growth rate and t is the duration of the interaction. For monochromatic, circularly polarized beams the duration of the interaction is given by the pump duration and has a growth rate $\gamma_0 = a_0(\omega_0\omega_p/2)^{1/2}$, where $a_0 = eA_0/mc$ is the normalized vector potential of the pump, with A_0 the vector potential amplitude. The large exponential growth possible has led to the suggestion of stimulated Raman backscattering in plasma as an alternative parametric amplifying medium[7] to conventional solid state laser media. In contrast to the RBS linear theory for long duration monochromatic beams, very interesting features appear when broad bandwidth chirped seed and pump pulses, with identical spectral bandwidths larger than twice the plasma frequency, are used. In this case, according to the Manley-Rowe relation,[8] energy flows from the pump to the seed when $\omega_0(z,t) - \omega_1(z,t) \approx \omega_p$ and from the seed to the pump when $\omega_1(z,t) - \omega_0(z,t) \approx \omega_p$. Furthermore, the chirp of the beams restricts the effective interaction duration, because the gain coefficient depends on detuning. Raman amplification only takes place when the detuning $\delta\omega = |\omega_0(z,t) - \omega_1(z,t) - \omega_p| \leq \gamma_0$, which reduces the interaction time to $\delta t = \pi\gamma_0/2\alpha$, and the overall amplitude growth becomes $g = e^{\pi\gamma_0^2/2\alpha}$, which is independent of time and where the chirp rate α, is such that $\omega_{0,1}(z,t) = \omega_0 + \alpha(t + z/c)$.[9,10] Assuming beams with a Gaussian profile, it can be shown analytically that each beam has maximum energy growth at $\omega \simeq \omega_0 - \omega_p$ (Stokes frequency) and

a)Electronic mail: g.vieux@strath.ac.uk.
b)Author to whom correspondence should be addressed. Electronic mail: d.a.jaroszynski@strath.ac.uk.

maximum loss at $\omega \simeq \omega_0 + \omega_p$ (anti-Stokes frequency). For the latter case, it requires that (i) $\pi|a_\omega|^2\omega\omega_p/2\alpha \ll 1$, where a_ω is the spectral amplitude at ω of the "so-called" pump beam, (ii) the pump profile remains almost unchanged during the energy exchange. Condition (ii) assumes that the "so-called" seed amplitude is much lower than the pump amplitude. In the following "seed" refers to the lower amplitude beam, which we identify as a diagnostic beam, while "pump" specifies the larger amplitude beam. The gain at $\omega_0 - \omega_p$ and loss at $\omega_0 + \omega_p$ are readily determined by measuring the ratio of the seed laser intensity spectrum $I'(\omega)$ after interaction with that of the initial spectrum $I(\omega)$, such that $g(\omega) = (I'(\omega) - I(\omega))/I(\omega)$. The separation between the two peaks is equal to twice the warm plasma frequency and leads directly to a measure of the density $n = (\omega_p^2\epsilon_0 m/e^2)^{1/2}$ after correcting for the plasma temperature. Furthermore, because the interaction time is limited to δt, a local measurement of the density at the position of the interaction is obtained. The timing of the collision instant is achieved by varying the delay between the two beams, which gives a measure of the spatio-temporal position where the density measurement is made. The range of plasma densities that can be measured is given by $\gamma_0 < \omega_p < \Delta\omega_{BW}/2$, where $\Delta\omega_{BW}$ represents the full spectral bandwidth of the laser pulse.

To confirm the feasibility of this method, we have carried out numerical simulations using the averaged 1D particle-in-cell (PIC) code aPIC,[11] which treats the laser field as a slowly varying quantity over a wavelength but calculates the full particle dynamics on a grid. We have modified aPIC to include spectral chirps. The simulated laser parameters are $a_{s0} = 1.8 \times 10^{-3}$ (seed amplitude) and $a_{p0} = 7.3 \times 10^{-3}$ (pump amplitude). All other laser parameters are identical, duration $\tau = 610$ fs, central wavelength $\lambda_0 = 800$ nm, spectral bandwidth $\Delta\lambda = 18$ nm. The plasma density, $n = 5 \times 10^{17}$ cm^{-3}, and temperature, $T = 5$ eV, have been chosen to coincide with our measured experimental parameters.[15] However, we have reduced the normalized vector potentials by a factor of 5 compared with the experimental values to ensure that the interaction remains in the linear RBS regime. 1D PIC codes overestimate the coupling and therefore the Raman gain. Figure 1 shows the gain curve obtained from the PIC simulation together with the expected gain curve from the analytic linear Raman theory. Good quantitative and qualitative agreement is achieved with energy gain and loss of a few percent observed on the red and blue side of the spectrum, respectively. The Stokes ω_G and anti-Stokes ω_L frequencies are easily extracted and after correcting for the plasma temperature, the cold plasma frequency is evaluated such that $\omega_{p(cold)} = ([(\omega_L - \omega_G)/2]^2 - 3(4\pi/\lambda_0)^2 Te/m)^{1/2}$, where $\omega_{p(cold)}^2 = \omega_{p(hot)}^2 - 3k_p^2 v_{th}^2$ is used, with v_{th} the electron thermal velocity. The value of n is recovered within an error of $\sim 1\%$.

To experimentally demonstrate this technique, the density of a plasma channel has been mapped out using broad-band Raman chirped pulse amplification. The experimental layout is presented in Figure 2. The plasma channel used has dual purpose as medium for the interaction and waveguide for the laser beam. The waveguide is formed by passing a high voltage discharge through a hydrogen filled capillary.[12] When the plasma cools against the wall of the capillary a parabolic radial density distribution, $n(r) = n(0) + \Delta n(r/r_m)^2$, develops,

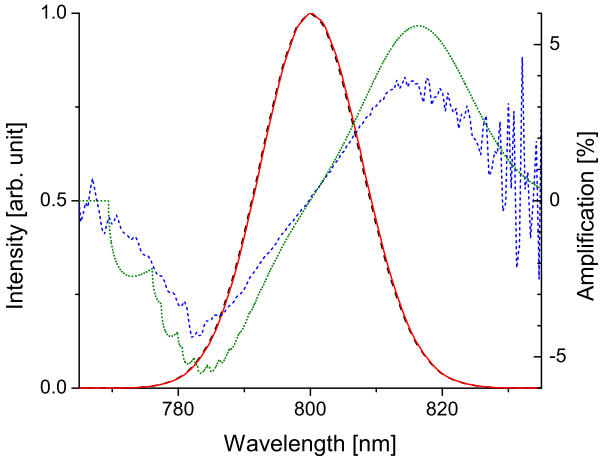

FIG. 1. 1D PIC results of a seed pulse interacting with a pump pulse in under-dense plasma. Dashed (black) line: initial seed spectrum, solid (red) line: seed spectrum after interaction, short-dashed (blue) line: gain curve from PIC simulation, dotted (green) line: expected gain curve from linear RBS theory.

where $n(0)$ is the on-axis density, and Δn is the density change between axis and boundary wall, r_m.[13] A Gaussian transverse mode laser beam couples to the fundamental mode of the waveguide when the beam waist $w_M = [r_m^2/(\pi r_e \Delta n)]^{1/4}$ (radius at $1/e^2$ of the intensity), where r_e is the classical electron radius. To study chirped pulse Raman amplification seed and pump laser beams, with M^2 parameter ≈ 2, from a Ti:sapphire laser system[14] with a central wavelength $\lambda = 800$ nm, and a full width at half maximum spectral bandwidth $\Delta\lambda_{FWHM} \approx 18$ nm, are focused, using two F/25 spherical mirrors, into either side of a 300 μm diameter, $L_c = 4$ cm long capillary filled with 70 mbar of hydrogen. The compressor is adjusted to produce 610 fs duration pulses. A MgF_2 beam splitter is used to partition the energy between the two beams: 90% serves as the pump while the remaining 10% is used for the seed. A transmission better than 80% through the capillary is obtained. A combination of quarter wave plates and polarizers in each beam line converts pump and seed to circular polarized beams while preventing feedback into the laser amplifier chain. A delay line in the seed beam line varies the relative time of injection of the seed into the plasma. It is thus possible to choose both the position and the time at which the density is measured. The beam energies at the entrance to the telescopes are 115 mJ (pump) and 5 mJ (seed), respectively, with

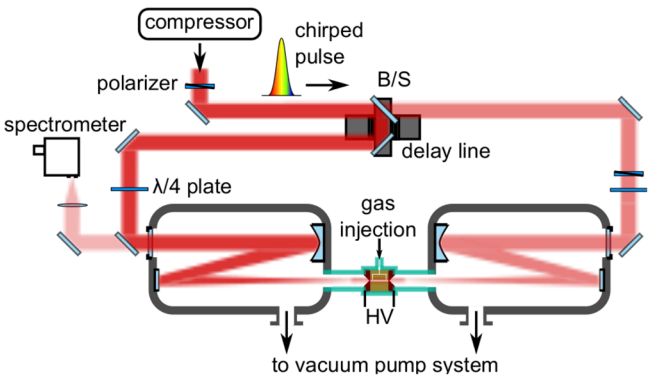

FIG. 2. Experimental schematic showing the counter-propagating circularly polarized pump and probe beams focused onto a plasma waveguide formed using an electrical discharge in hydrogen gas.

corresponding focal spot sizes of 55 μm and 65 μm. These give intensities of 1.4×10^{15} and 8.6×10^{13} Wcm^{-2}, which corresponds to normalized vector potentials $a_{p0} = 1.8 \times 10^{-2}$ and $a_{s0} = 4.5 \times 10^{-3}$, respectively. Both the seed and pump are linearly chirped at a rate $\alpha = 8.66 \times 10^{25}$ rads^{-2}. The theoretical growth rate is $\gamma_0 \approx 4 \times 10^{12}$ rads^{-1}, which limits the duration of the interaction to $\delta t = 78$ fs, representing a distance of 23 μm. Radiation transmitted through a high reflective mirror is focused into a spectrometer and the seed spectra are measured with and without the presence of the pump in the channel. To improve the signal to noise ratio, 40 spectra are recorded and averaged for a single acquisition, and up to 5 measurements performed at each position. It should be noted that the primary goal of this experiment was not to measure the plasma density and therefore condition (i) is only approximately satisfied, and an error ($\sim$30%) on the density measurements is expected. However, these measurements are valid for a proof-of-principle demonstration of the method.

$g(\omega)$ is calculated as presented earlier and typical spectra and gain curve are shown in Figure 3. Clear Stokes and anti-Stokes satellites are visible in agreement with the analytical and simulation results. Values of the Stokes and anti-Stokes wavelengths measured as function of the relative delay between the two beams are shown in Figure 4. In this set of measurements, both satellites are present simultaneously and at all times. It is observed that the Stokes wavelength is constant at $\approx$817 nm for the majority of delays. Its value decreases steepily at both ends of the measurement range, which is consistent with the decrease in density at the ends of the capillary. If we examine the wavelengths for the anti-Stokes satellite, we notice that they fluctuate around a constant value of $\approx$783 nm. The net result is that the frequency difference between the Stokes and anti-Stokes satellites is constant over most of the measurement range, suggesting that the electron plasma density is also constant over much of that length. Figure 5 shows the electron density calculated from the frequency difference between the Stokes and anti-Stokes satellites corrected for the 3 eV plasma temperature, which agrees with the density and temperature determined using spectroscopy methods.[15] As expected, the density, within the experimental error, is constant inside the capillary and decreases at the extremities. The measured on-axis density is evaluated to be $7 - 8 \times 10^{17}$ cm^{-3} between the two gas inlets. Interestingly, the length over which the density is high extends beyond 40 mm because of the plasma plume. We also observe that the density drops off more rapidly at the entrance to the capillary than at the exit, which we ascribe to laser micro-machining by the pump enlarging the entrance diameter. To compare, the density determined from the frequency difference between the laser central frequency and the Stokes frequencies gives $\approx 7 \times 10^{17}$ cm^{-3} at the centre of the capillary, which is in close agreement with our previous averaged measurements.[10] We have estimated that the maximum plasma density that can be measured because of the finite width of the laser spectrum is $n \approx 10^{18}$ cm^{-3}. To verify that the density varies with backing pressure, a pressure scan was performed at the fixed position $l = 36$ mm, as shown in Figure 6. To measure higher densities larger bandwidth pulses are required. The density increases linearly with backing pressure at higher pressures, as expected. However, at the lowest pressure, the density is smaller than expected because of minor gas leaks in the gas feed line. These results indicate that for our laser parameters the lowest measurable

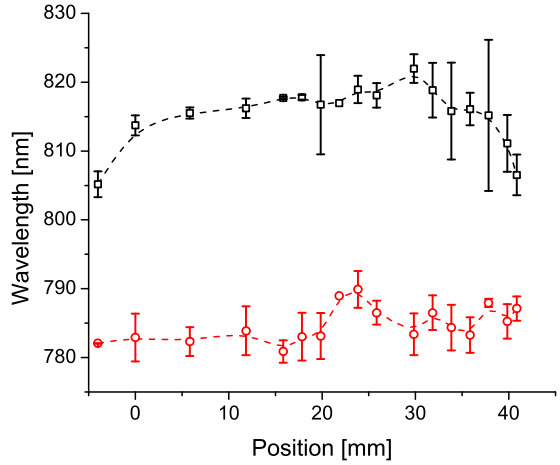

FIG. 4. Measurements of the Stokes (square) and anti-Stokes (circle) wavelengths as a function of the relative delay between the two laser beams.

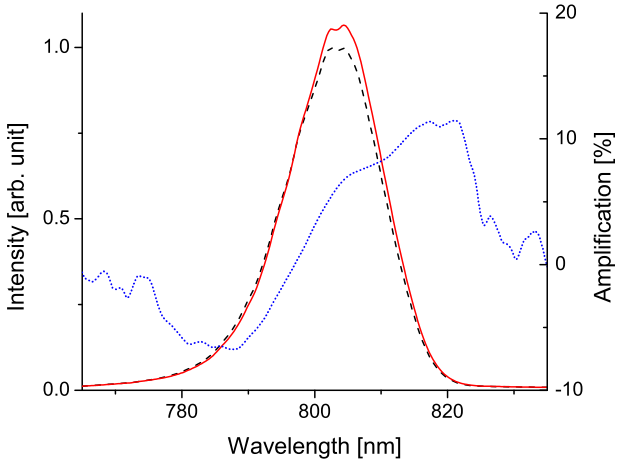

FIG. 3. A typical measurement representing an average of 40 spectra. Dashed (black) curve: spectrum without interaction with pump beam, solid (red) line: spectrum after interaction with pump beam, dotted (blue) line: gain curve.

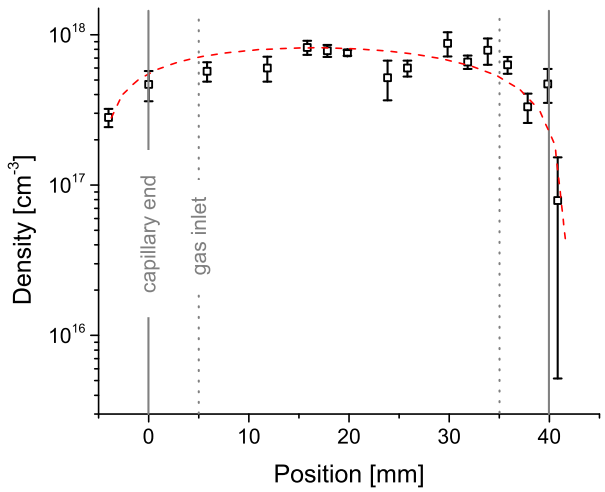

FIG. 5. Density values calculated from the frequency difference between the Stokes and anti-Stokes satellites.

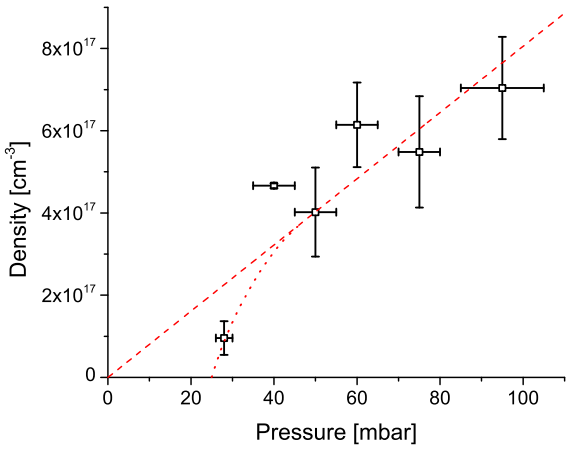

FIG. 6. Density measured as a function of backing pressure. The dashed line is a linear fit of the experimental data. The dotted line is a guide for the eye, showing the non linear behaviour of the density change at low backing pressure.

density is around $10^{17}\,\mathrm{cm}^{-3}$, which is similar to the lowest densities measured in Figure 5.

In conclusion, we have shown that RBS can be used as a diagnostic tool to measure local plasma density. Experimental implementation is relatively easy; it does not require the use of an external beam, because the seed beam is provided by a pick off of the main beam; and finally the density is determined directly from the measured spectra. The length of a 40 mm long capillary, for which no transverse illumination is possible, was probed longitudinally using two counter-propagating, short, chirped laser pulses. A plasma density of $7-8\times10^{17}\,\mathrm{cm}^{-3}$ was measured over a large fraction of the plasma channel and density variation in the plasma plumes at the exits of the capillary was also measured. The lower and upper limits of the measurable density for our laser parameters are 10^{17} and $10^{18}\,\mathrm{cm}^{-3}$, respectively. Due to the two beam nature of this technique, just above threshold laser intensities for RBS are sufficient to obtain a measurement, thus leaving the plasma largely undisturbed.

We gratefully acknowledge the support of the EPSRC, UK, the EC's LASERLAB-EUROPE/LAPTECH (No. 284464), the EUCARD-2 project (No. 312453) and the technical support of David Clark, without which the work presented here would not have been possible.

[1]S. H. Lam, Phys. Fluids **8**, 73 (1965).
[2]D. E. Evans and J. Katzenstein, Rep. Prog. Phys. **32**, 207 (1969).
[3]M. D. Perry, C. Darrow, C. Coverdale, and J. K. Crane, Opt. Lett. **17**, 523 (1992).
[4]T. Weineisen, B. Goeppner, K. Schmid, M. Fuchs, H. Schroeder, S. Karsch, and F. Gruener, Phys. Rev. ST Accel. Beams **14**, 050705 (2011).
[5]H. Jang, M. S. Hur, J. M. Lee, M. H. Cho, W. Namkung, and H. Suk, Appl. Phys. Lett. **93**, 071506 (2008).
[6]W. L. Kruer, *The Physics of Laser Plasma Interactions* (Addison-Wesley, New York, 1988).
[7]G. Shvets, N. J. Fisch, A. Pukhov, and J. Meyer ter Vehn, Phys. Rev. Lett. **81**, 4879 (1998); V. M. Malkin, G. Shvets, and N. J. Fisch, Phys. Plasmas **7**, 2232 (2000).
[8]M. Manley and H. E. Rowe, Proc. IRE **44**, 904 (1956).
[9]B. Ersfeld and D. A. Jaroszynski, Phys. Rev. Lett. **95**, 165002 (2005).
[10]G. Vieux, A. Lyachev, X. Yang, B. Ersfeld, J. P. Farmer, E. Brunetti, R. C. Issac, G. Raj, G. H. Welsh, S. M. Wiggins, and D. A. Jaroszynski, New J. Phys. **13**, 063042 (2011).
[11]M. S. Hur, G. Penn, J. S. Wurtele, and R. Lindberg, Phys. Plasmas **11**, 5204 (2004).
[12]D. J. Spence, A. Butler, and S. M. Hooker, J. Opt. Soc. Am. B **20**, 138 (2003).
[13]D. J. Spence, P. D. S. Burnett, and S. M. Hooker, Opt. Lett. **24**, 993 (1999); D. J. Spence and S. M. Hooker, Phys. Rev. E **63**, 015401 (2000).
[14]D. A. Jaroszynski, B. Ersfeld, G. Giraud, S. Jamison, D. R. Jones, R. C. Issac, B. M. W. McNeil, A. D. R. Phelps, G. R. M. Robb, H. Sandison, G. Vieux, S. M. Wiggins, and K. Wynne, Nucl. Instrum. Methods Phys. Res. A **445**, 317 (2000).
[15]S. Abuazoum, S. M. Wiggins, B. Ersfeld, K. Hart, G. Vieux, X. Yang, G. H. Welsh, R. C. Issac, M. P. Reijnders, D. R. Jones, and D. A. Jaroszynski, Appl. Phys. Lett. **100**, 014106 (2012).